

Aerosol Ion Characteristics During the Big Bend Regional Aerosol and Visibility Observational Study

Taehyoung Lee, Sonia M. Kreidenweis, and Jeffrey L. Collett, Jr.

Department of Atmospheric Science, Colorado State University, Fort Collins, Colorado

ABSTRACT

The ionic compositions of particulate matter with aerodynamic diameter $\leq 2.5 \mu\text{m}$ ($\text{PM}_{2.5}$) and size-resolved aerosol particles were measured in Big Bend National Park, Texas, during the 1999 Big Bend Regional Aerosol and Visibility Observational study. The ionic composition of $\text{PM}_{2.5}$ aerosol was dominated by sulfate (SO_4^{2-}) and ammonium (NH_4^+). Daily average SO_4^{2-} and NH_4^+ concentrations were strongly correlated ($R^2 = 0.94$). The molar ratio of NH_4^+ to SO_4^{2-} averaged 1.54, consistent with concurrent measurements of aerosol acidity. The aerosol was observed to be comprised of a submicron fine mode consisting primarily of ammoniated SO_4^{2-} and a coarse particle mode containing nitrate (NO_3^-). The NO_3^- appears to be primarily associated with sea salt particles where chloride has been replaced by NO_3^- , although formation of calcium nitrate ($\text{Ca}(\text{NO}_3)_2$) is important, too, on several days. Size-resolved aerosol composition results reveal that a size cut in particulate matter with aerodynamic diameter $\leq 1 \mu\text{m}$ would have provided a much better separation of fine and coarse aerosol modes than the standard $\text{PM}_{2.5}$ size cut utilized for the study. Although considerable nitric acid exists in the gas phase at Big Bend, the aerosol is sufficiently acidic and temperatures sufficiently high that even significant future reductions in $\text{PM}_{2.5}$ SO_4^{2-} are unlikely to be offset by formation of particulate ammonium nitrate in summer or fall.

IMPLICATIONS

Aerosol particles in Big Bend National Park during summer and fall include an external mixture of submicron, acidic partially ammoniated SO_4^{2-} particles and supermicron sodium nitrate or $\text{Ca}(\text{NO}_3)_2$ particles. The NO_3^- is present as a result of reactions of nitric acid or its precursors with sea salt or soil dust. The division between the two aerosol modes is at $\sim 1 \mu\text{m}$, such that $\text{PM}_{2.5}$ samples include a significant part of the coarse mode tail. The acidity of the SO_4^{2-} aerosol and the importance of sodium nitrate and $\text{Ca}(\text{NO}_3)_2$ particles should be considered when examining aerosol hygroscopicity and aerosol contributions to regional haze.

INTRODUCTION

The Big Bend Regional Aerosol and Visibility Observational (BRAVO) study was conducted in the region surrounding Big Bend National Park during 4 months from July to October, 1999. Despite its remote location, Big Bend National Park frequently experiences poor visibility caused by long-range pollutant transport.¹ Big Bend National Park, located on the Rio Grande River on the Texas–Mexico border, is designated a Class I area.^{2,3} The Interagency Monitoring of Protected Visual Environments (IMPROVE) network and earlier networks have included measurements at Big Bend since 1982.

A 1996 study found that sulfate (SO_4^{2-}) was the major contributor to fine particle mass and the largest contributor to visibility degradation in Big Bend National Park.⁴ The highest fine particulate SO_4^{2-} concentrations were observed in summer and autumn; however, no information was available from this earlier study regarding the size distribution or acidity of the SO_4^{2-} aerosol. The size of the SO_4^{2-} particles has a strong effect on their light-scattering efficiency. Likewise, the acidity of the SO_4^{2-} aerosol strongly affects its hygroscopicity and, hence, the amount of water on the particles at a given humidity. More acidic forms of SO_4^{2-} (e.g., ammonium bisulfate [NH_3HSO_4], letovicite, or sulfuric acid [H_2SO_4]) take up liquid water at much lower relative humidities than ammonium sulfate ($(\text{NH}_4)_2\text{SO}_4$).^{5–7} Addition of water to SO_4^{2-} -containing particles is an important factor governing their masses and scattering efficiencies and, therefore, their impact on visibility degradation.

Organic carbon and soil-derived aerosol particles were observed to contribute significantly to visibility degradation in Big Bend National Park as well, although their contributions were typically much smaller than that observed for SO_4^{2-} .¹ The highest contributions of organic carbon are observed during the spring when agriculture-related biomass burning in Mexico is suspected to be a primary source.^{4,8} The presence of soil and dust particles was associated with local emissions as well as with suspected Saharan dust episodes in July and August.⁴

To improve understanding of the visibility-degrading properties and sources of aerosol particles in Big Bend

National Park, the 4-month BRAVO study was conducted during summer and fall 1999. As part of BRAVO, a series of special aerosol characterization studies was conducted in the park itself to provide detailed information about the physical and chemical properties of the aerosol particles. These included a determination of the particle size distribution,⁹ characterization of the organic composition of the aerosol,¹⁰ and a detailed investigation of aerosol ionic chemical composition. The objective of this work is to examine the aerosol ionic chemical composition, focusing on examination of aerosol acidity, major ion concentrations in particulate matter with aerodynamic diameter $\leq 2.5 \mu\text{m}$ ($\text{PM}_{2.5}$), and aerosol ion size distributions.

EXPERIMENTAL PROCEDURES

The BRAVO study (www2.nature.nps.gov/ait/studies/bravo/index.html) was conducted during July 1–October 31, 1999. A network of ~ 40 sites was used to measure aerosol properties following the IMPROVE protocol. More detailed measurements of aerosol composition were conducted at the K-Bar ranch site inside Big Bend National Park.

Concentrations of aerosol ions at the K-Bar site were measured in daily 24-hr $\text{PM}_{2.5}$ samples collected with an annular denuder/filter-pack system manufactured by URG. Ambient air was drawn through a cyclone ($D_{50} = 2.5 \mu\text{m}$) and through two coated annular denuders (242 mm) in series to collect the gaseous species of interest. Sodium chloride (NaCl [0.1%]) coated the first denuder for collection of nitric acid (HNO_3), and the second denuder was coated with 0.5 g citric acid in 50 mL of methanol to collect ambient ammonia (NH_3). Pre-filter collection of NH_3 helps preserve acidic aerosol samples.¹¹ The remaining airstream was then filtered through 47-mm diameter Teflon and nylon filters in series. The Teflon filter (Gelman Teflo, 2- μm pore size) was used to collect particulate matter (PM). The nylon membrane filter (Gelman Nylasorb) was used to capture any HNO_3 volatilized from PM on the Teflon filter. Samples were collected from 8:00 a.m. to 8:00 p.m. central daylight time with a nominal flow rate of 10 L/min. Flow was controlled by a mass flow controller and the actual sample volume was monitored using a dry gas meter with appropriate correction for system pressure drop. Two URG systems were operated to permit rapid daily sample changeover, collection of replicate samples (on selected days), and regular collection of system blanks.

Daily 24-hr impactor samples were also collected using a Micro-Orifice Uniform Deposit Impactor (MOUDI). The largest eight stages of the MOUDI were used, corresponding to the following aerodynamic diameter size ranges: 18–10 μm , 10–5.6 μm , 5.6–3.2 μm , 3.2–1.8 μm , 1.8–1 μm , 1–0.56 μm , 0.56–0.32 μm , and 0.32–0.18 μm .

Additionally, there was an initial stage that collected particles with aerodynamic diameter $>18 \mu\text{m}$. The MOUDI stages used in the study were selected to provide good coverage of the expected ion size distributions and to avoid potential clogging issues associated with use of stages with smaller size cuts. Samples were collected on greased aluminum foil impaction surfaces¹² to reduce particle bounce. The MOUDI impactor was operated 6 days each week, with the seventh day used for impactor cleaning and collection of a sampler blank.

Analysis of the collected aerosol samples focused on quantification of the main ionic species: chloride (Cl^-), SO_4^{2-} , nitrate (NO_3^-), sodium (Na^+), ammonium (NH_4^+), potassium (K^+), magnesium (Mg^{2+}), and calcium (Ca^{2+}). $\text{PM}_{2.5}$ and denuder samples were extracted and analyzed on-site to minimize potential artifacts (e.g., neutralization) associated with sample storage and shipping. Samples were loaded and unloaded in an NH_3 -free glove box to further minimize potential artifact neutralization. Ion analysis was completed on two Dionex DX-500 ion chromatographs set up in a trailer at the field site. A Dionex AG4A-SC guard column, an AS4A-SC separation column, and a self-regenerating anion suppressor were used to measure anion concentrations. Cations were measured using a Dionex CG12A guard column, a CS12A separation column, and a self-regenerating cation suppressor. Detection was by conductivity in both cases. Both ion chromatographs were calibrated daily using a series of standards prepared from analytical-grade salts. Replicate injections and analysis of independent National Institute of Science and Technology-traceable standards were used to establish measurement precision and accuracy.

$\text{PM}_{2.5}$ and denuder samples were generally extracted twice per week, with cation and anion analyses usually conducted once per week. Denuders were extracted with 10 mL deionized water freshly prepared on-site. The nylon membrane filter was extracted using 6 mL of ion chromatographic anion eluent (1.8 mM sodium carbonate (Na_2CO_3)/1.7 mM NaHCO_3). Each Teflo filter was extracted with 5.85 mL of 10^{-4} N perchloric acid (HClO_4) solution with 150 μL of ethanol added first to wet the filter. pH measurements (Orion model 250A portable pH meter equipped with a Ross Sure-Flow combination pH electrode calibrated with pH 4 and 7 buffers and a series of H_2SO_4 solutions) of the $\text{PM}_{2.5}$ extracts were made immediately after extraction to measure strong aerosol acidity. The background acidity from the HClO_4 extract solution inhibits dissolution of carbon dioxide (CO_2) and other weak acids to permit measurement of sample strong acidity. The hydrogen ion (H^+) concentration of a filter blank was subtracted from each filter extract concentration to determine the aerosol strong acidity contribution.

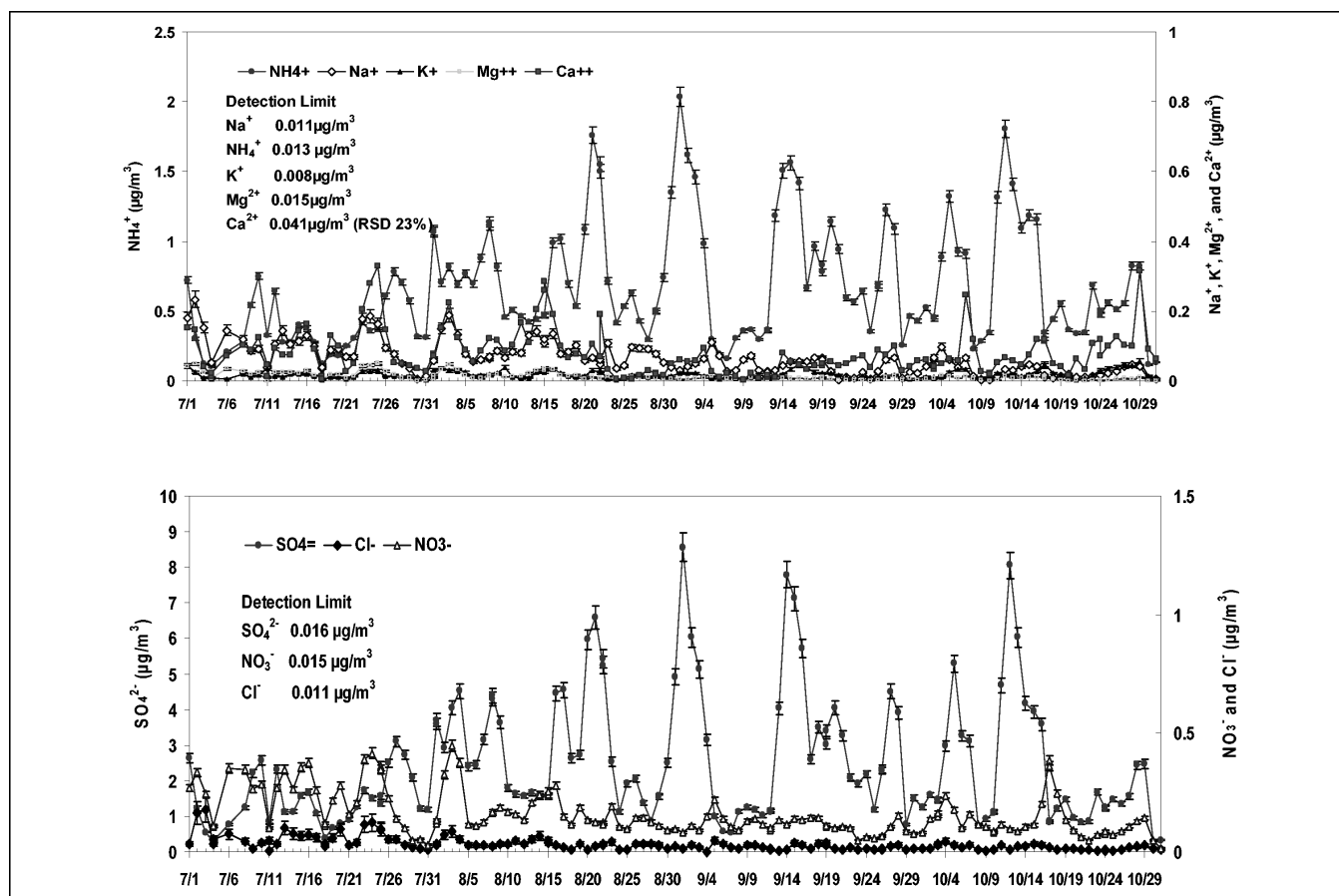


Figure 1. Timelines of major $PM_{2.5}$ ion concentrations. The error bars represent measurement precision (1 standard deviation).

MOUDI samples were stored frozen until later analysis in the laboratory at Colorado State University. Samples from 41 study days (plus several blanks) were analyzed. This subset of sample periods was selected based on interesting $PM_{2.5}$ aerosol composition measurements (e.g., high SO_4^{2-} , high NO_3^- , and suspected sea-salt days) and other BRAVO study results (particle size distributions and thermodynamic modeling studies). MOUDI impactor substrates were extracted by sonication in deionized water ($HClO_4$ was not needed because acidity measurements were not made on these samples) and analyzed using the same ion chromatograph systems and approaches outlined previously.

Analysis of sample replicates and blanks permitted establishment of measurement precision and detection limits. Precisions for the major measured aerosol species (NO_3^- , SO_4^{2-} , NH_4^+ , and H^+) were good with relative standard deviations (RSDs) in the range of 3–5%. RSDs for trace aerosol ions were higher, ranging from 12 to 23%. RSDs for replicate denuder measurements of HNO_3 and NH_3 were each 9%. RSDs for replicate sample analyses of MOUDI extracts were all below 6%.

$PM_{2.5}$ NO_3^- concentrations are reported as the sum of NO_3^- measured on the Teflon and the backup nylon filter. Further details of all sampling and analysis

protocols, including copies of study Standard Operating Procedures are presented by Lee and Collett.¹³

RESULTS AND DISCUSSION

Study timelines of the major $PM_{2.5}$ ions and a statistical summary of concentrations of $PM_{2.5}$ ion components and gases are presented in Figure 1 and Table 1, respectively. SO_4^{2-} and NH_4^+ were the dominant ionic species in daily $PM_{2.5}$, with smaller contributions from NO_3^- , Na^+ , and

Table 1. Statistical summary of $PM_{2.5}$ and gas compositions ($\mu g/m^3$) measured using the URG sampler.

Species	Mean	Min	Max	Standard Deviation
HNO_3 (g)	0.545	1.555	0.084	0.341
NH_3 (g)	0.156	0.003	0.624	0.131
Cl^- (p)	0.033	0.002	0.177	0.029
SO_4^{2-} (p)	2.391	0.289	8.568	1.751
NO_3^- (p)	0.159	0.015	0.451	0.093
Na^+ (p)	0.063	0.002	0.234	0.047
NH_4^+ (p)	0.651	0.102	2.037	0.415
K^+ (p)	0.018	0.002	0.055	0.011
Mg^{2+} (p)	0.013	0.001	0.052	0.012
Ca^{2+} (p)	0.082	0.003	0.329	0.068
H^+ (p) (nmol/m ³)	13.08	0	75.56	14.27

other species. SO_4^{2-} concentrations were highest in the period from August to October, reaching as high as $8.5 \mu\text{g}/\text{m}^3$. Daily average SO_4^{2-} and NH_4^+ concentrations were strongly correlated ($R^2 = 0.94$) as shown in Figure 2. $\text{PM}_{2.5}$ NO_3^- and SO_4^{2-} concentrations showed little correlation ($R^2 = 0.05$).

The aerosol was usually acidic, with an average $\text{PM}_{2.5}$ NH_4^+ to SO_4^{2-} molar ratio of 1.54 (standard deviation of 0.3). The ratios of NH_4^+ to SO_4^{2-} showed a trend consistent with the aerosol acidity measurements (see Figure 3). A high correlation between SO_4^{2-} and H^+ was observed ($R^2 = 0.9$) as shown in Figure 4. The average acidity measured during BRAVO was $13 \text{ nmol H}^+/\text{m}^3$ with a range of $0\text{--}75.6 \text{ nmol}/\text{m}^3$. These values are similar to aerosol acidities measured in previous midwestern U.S. studies in Portage, WI (average = $8 \text{ nmol}/\text{m}^3$, range = $0\text{--}78 \text{ nmol}/\text{m}^3$), St. Louis, MO ($10, 0\text{--}122 \text{ nmol}/\text{m}^3$), and Chicago, IL ($7.7, 0\text{--}78 \text{ nmol}/\text{m}^3$),^{14–17} but somewhat lower than measured at eastern U.S. sites in Kingston, TN ($36.1, 0\text{--}290 \text{ nmol}/\text{m}^3$) and Boston, MA ($17.9, 1.3\text{--}84 \text{ nmol}/\text{m}^3$).^{18,19} The most acidic BRAVO aerosol was observed during August, September, and the beginning of October, with 24-hr average concentrations in the range of $40\text{--}80 \text{ nmol}/\text{m}^3$ of H^+ on several days.

Both NO_3^- and NH_4^+ can partition between the gas and particle phases. The sum of gaseous NH_3 and particulate NH_4^+ comprise N in the minus three oxidation state (N(-III)). Likewise, the sum of gaseous HNO_3 and particulate NO_3^- comprise N(V). N(V) and N(-III) were found to exhibit quite different distributions between the particle and gas phases (see Figure 5). The average ratio for $\text{HNO}_3(\text{g})/\text{N}(\text{V})$ was 0.73 and for $\text{NH}_3(\text{g})/\text{N}(\text{-III})$ was 0.22. (These ratios do not reflect NO_3^- or NH_4^+ contained in particles with aerodynamic diameters larger than $2.5 \mu\text{m}$.)

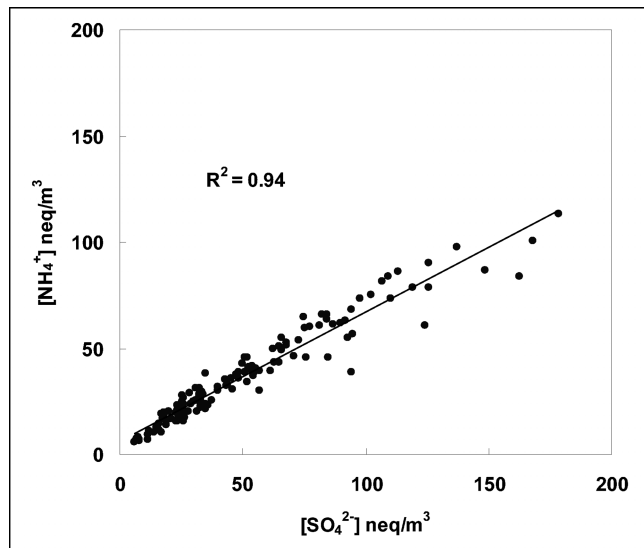


Figure 2. Relationship between NH_4^+ and SO_4^{2-} concentrations in BRAVO $\text{PM}_{2.5}$ aerosol.

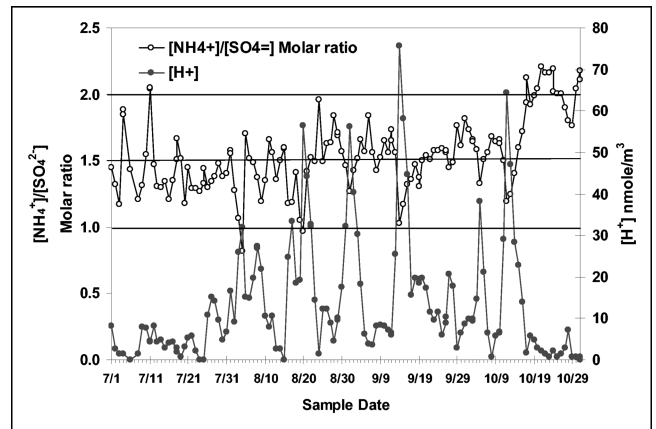


Figure 3. Timelines of the molar ratio of $\text{NH}_4^+/\text{SO}_4^{2-}$ and the $\text{PM}_{2.5}$ H^+ concentration. As reference, horizontal lines are included at $\text{NH}_4^+/\text{SO}_4^{2-}$ molar ratios of 1, 1.5, and 2 corresponding to the compositions of $(\text{NH}_4)_2\text{SO}_4$, letovicite, and NH_4HSO_4 , respectively.

The implication is that most of the available N(-III) has been taken up into particles, while the majority of N(V) remains in the gas phase, representing potential for formation of additional particulate NO_3^- .

Back trajectory analysis revealed that days with high HNO_3 concentrations featured quite different transport from days with high $\text{PM}_{2.5}$ NO_3^- . High HNO_3 days were generally also high SO_4^{2-} days and typically featured transport from a sector extending east-southeast to northeast of Big Bend National Park. High $\text{PM}_{2.5}$ NO_3^- days, in contrast, typically featured transport from the southeast and across the Gulf of Mexico. These transport differences suggest that $\text{PM}_{2.5}$ NO_3^- concentrations are governed not by HNO_3 availability but by some other factor that promotes NO_3^- particle formation.

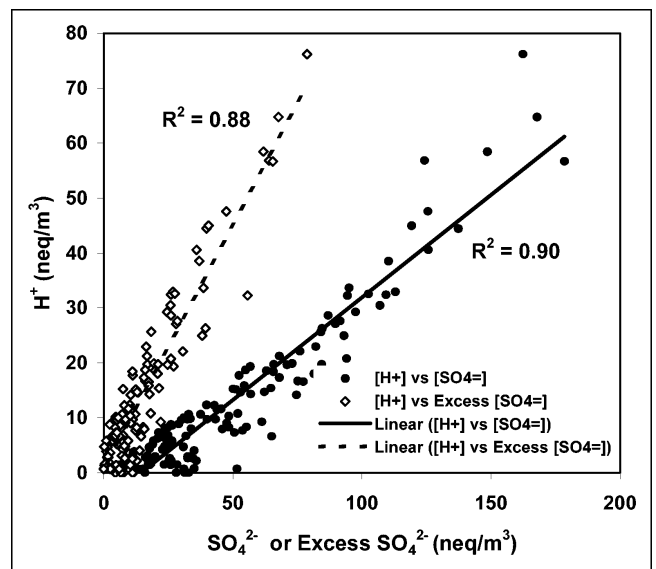


Figure 4. Relationships between H^+ and SO_4^{2-} and between H^+ and excess SO_4^{2-} in BRAVO $\text{PM}_{2.5}$ aerosol.

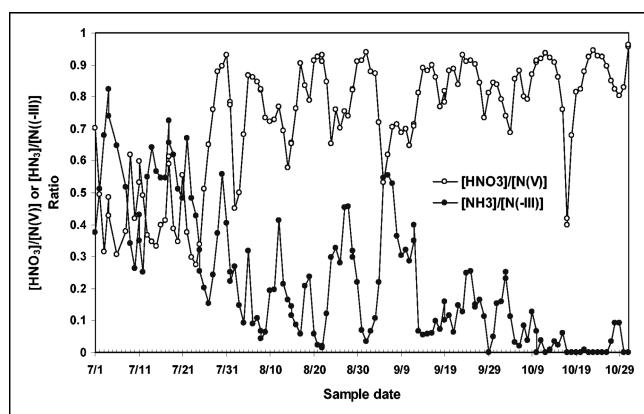


Figure 5. Timelines of ratios of $\text{HNO}_3/\text{N(V)}$ and $\text{NH}_3/\text{N(-III)}$. The particle components of N(V) and N(-III) in these ratios only include material measured in the $\text{PM}_{2.5}$ fraction.

Comparison of $\text{PM}_{2.5}$ Na^+ and Cl^- concentrations (see Figure 6) reveals that the observed Cl^-/Na^+ equivalent ratio (average ~ 0.33) is much lower than expected for sea salt (~ 1.16).²⁰ The combination of apparent Cl^- loss from sea salt and the observation that $\text{PM}_{2.5}$ NO_3^- concentrations peak during periods with transport from the Gulf region, suggests that HNO_3 reaction with sea salt is important. Indeed, if we examine the daily ratios of the sum of $\text{PM}_{2.5}$ NO_3^- and Cl^- to $\text{PM}_{2.5}$ Na^+ , it is found that on many days they fall close to the ratio expected in aged sea salt (see Figure 6). This is consistent with the reaction of HNO_3 with sea salt, resulting in a stoichiometric loss of volatilized hydrochloric acid.²¹ The correlation between NO_3^- and Na^+ is moderate ($R^2 = 0.64$), further suggesting the presence of sea salt aerosol as an important precursor to particulate NO_3^- formation in this environment. A weaker correlation was observed between NO_3^- and Ca^{2+}

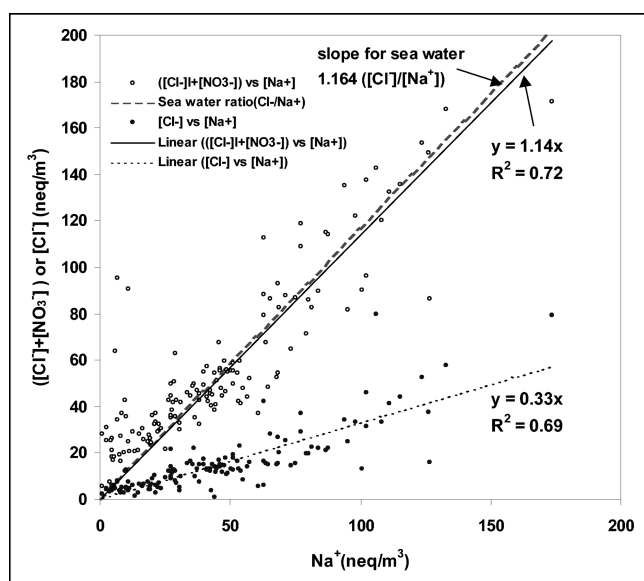


Figure 6. Relationship between Na^+ and Cl^- and between Na^+ and the sum of NO_3^- and Cl^- .

($R^2 = 0.33$), suggesting that HNO_3 condensation onto dust particles might also exert some influence on aerosol NO_3^- formation. Occurrence of this reaction can account for why some ratios of $(\text{NO}_3^- + \text{Cl}^-)$ to Na^+ fall above the sea salt line. This becomes clearer if the data are replotted as shown in Figure 7. Here, the observed ratio of $(\text{Cl}^- + \text{NO}_3^-)/\text{Na}^+$ is compared with the expected Cl^-/Na^+ sea salt ratio (shown as a horizontal line) as a function of the observed $\text{Ca}^{2+}/\text{Na}^+$ ratio. When the $\text{Ca}^{2+}/\text{Na}^+$ ratio is high, indicating a greater presence of dust than sea salt, the $(\text{NO}_3^- + \text{Cl}^-)/\text{Na}^+$ ratio tends to fall well above the sea salt ratio line, indicating that much more NO_3^- is present than can be accounted for by HNO_3 reaction with sea salt. Presumably, this reflects formation of $\text{Ca}(\text{NO}_3)_2$ or other HNO_3 -dust reaction products. Recent laboratory tests²² have demonstrated that reaction of HNO_3 with CaCO_3 particles occurs with a timescale on the order of hours, even at relative humidities as low as 17%. When the $\text{Ca}^{2+}/\text{Na}^+$ ratio is lower than ~ 3 , indicating increased presence of sea salt (relative to dust), the points mainly fall close to the line, indicating that most NO_3^- probably is associated with reacted sea salt particles.

Further insight into the properties of BRAVO aerosol NO_3^- , as well as other species, is possible through examination of the MOUDI impactor results. Figure 8 depicts the average measured size distributions for SO_4^{2-} , NH_4^+ , NO_3^- , Cl^- , Na^+ , K^+ , Mg^{2+} , and Ca^{2+} . These average distributions are representative of the general features of the distributions measured on the 41 selected MOUDI analysis days, although observed concentrations of the different ions changed (sometimes significantly) from day

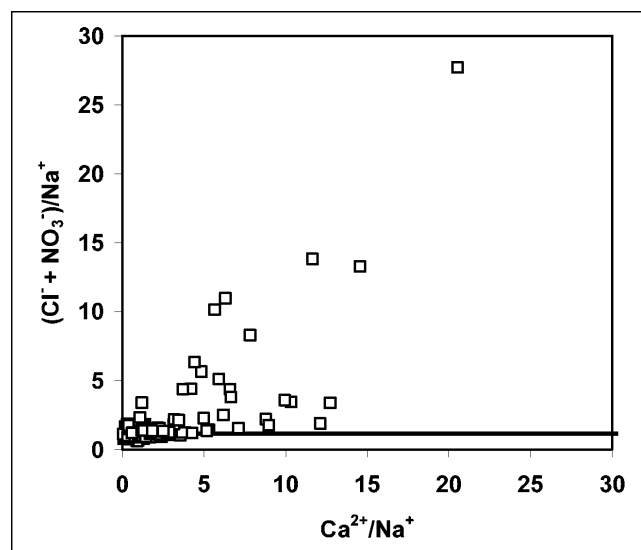


Figure 7. Comparison of the ratio of $(\text{NO}_3^- + \text{Cl}^-)/\text{Na}^+$ with the sea salt Cl^-/Na^+ ratio (indicated as horizontal line) as a function of the $\text{Ca}^{2+}/\text{Na}^+$ ratio. The figure does not include one sample at a $\text{Ca}^{2+}/\text{Na}^+$ ratio of 51, which also falls well above the sea salt ratio line. Units used for all species in these ratios were neq/m^3 .

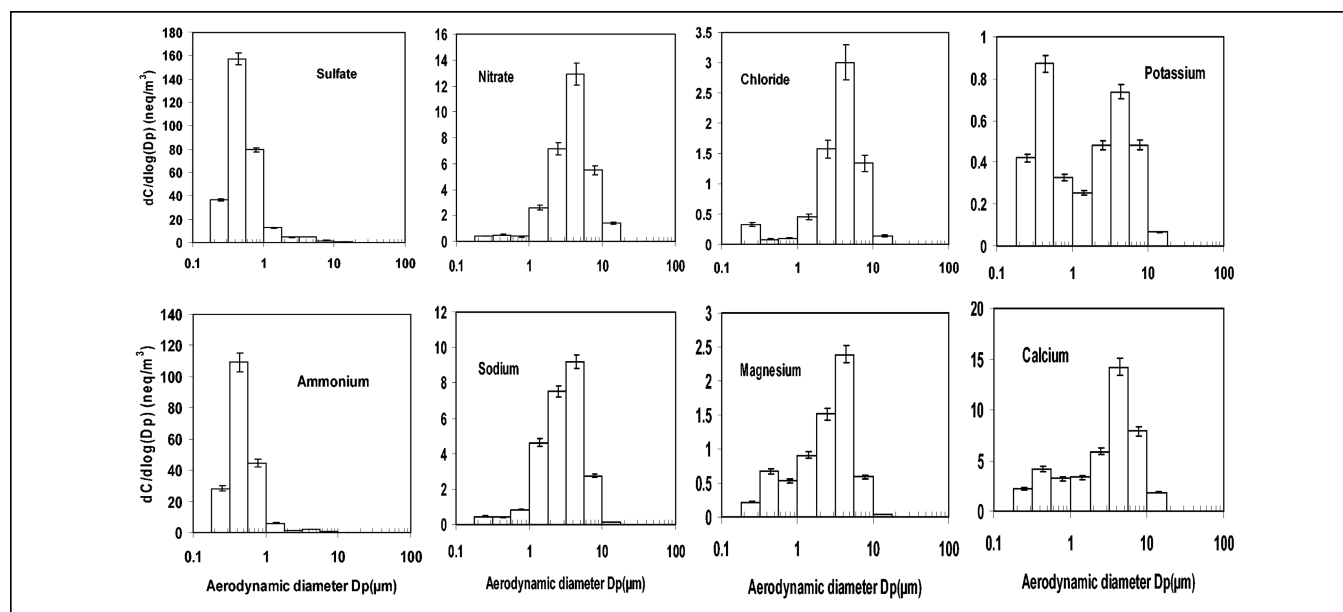


Figure 8. The average measured size distributions of inorganic ion concentrations. The error bars represent analytical precision (1 standard deviation).

to day. Integrated results for the submicron aerosol species (NH_4^+ and SO_4^{2-}) from the appropriate stages of the MOUDI impactor show excellent agreement with $\text{PM}_{2.5}$ concentrations measured using the URG sampler, providing confidence in the quality of the two data sets. A direct comparison is not possible for the other species, which are distributed over a broader size range, because of the lack of matching size cuts between the $\text{PM}_{2.5}$ sampler and MOUDI impactor, where the closest size cut is at $3.2 \mu\text{m}$.

The MOUDI SO_4^{2-} and NH_4^+ size distributions exhibit very similar shapes, with a submicron mode typically peaked at $0.4\text{--}0.5 \mu\text{m}$ aerodynamic diameter. NO_3^- , by contrast, is found almost exclusively in a coarse particle mode, with a characteristic mode diameter of $\sim 4\text{--}5 \mu\text{m}$. (There are some days near the end of October where a small fine particle mode of what appears to be NH_4NO_3 was also observed; the presence of NH_4NO_3 during this period is consistent with the observation that the $\text{NH}_4^+/\text{SO}_4^{2-}$ molar ratio climbed slightly above 2 (see Figure 3). The average NO_3^- size distribution has a shape very similar to the size distributions of sea salt components Na^+ and Cl^- , further supporting the interpretation that particulate NO_3^- in BRAVO was formed primarily as a result of HNO_3 (or other precursor nitrogen species) reaction with sea salt particles. Several days, however, were observed when the amount of NO_3^- found in coarse particles considerably exceeded the amount of Na^+ . On these days, sufficient Ca^{2+} was present to account for the NO_3^- , consistent with the analysis presented in Figure 7. The bimodal nature of the average K^+ distribution is also interesting. Individual day samples in the first half of the study tended to contain mostly coarse-mode K^+ , while distributions from days in September and October frequently contain both fine- and coarse-mode K^+ .

The findings from the MOUDI size distribution measurements have several important implications. First, the coexistence of acidic, submicron ammoniated SO_4^{2-} particles with coarse-mode sea salt, reacted sea salt (NaNO_3), and dust particles indicates the aerosol is externally mixed, even within the $\text{PM}_{2.5}$ fraction. Second, the commonly made assumption that fine particle NO_3^- is present mainly as NH_4NO_3 ^{2,3} is clearly not appropriate for BRAVO aerosol. The fact that the NO_3^- is present mainly in the form of coarse-mode NaNO_3 particles is important for understanding the hygroscopicity and refractive index of NO_3^- containing particles in this environment, topics addressed in some detail by Malm et al.²³ Significant formation of hygroscopic $\text{Ca}(\text{NO}_3)_2$ ²² on some days is also of interest. Third, the MOUDI ion distribution measurements clearly show that a size cut at $1 \mu\text{m}$ aerodynamic diameter would provide a much better separation of the coarse and fine particle modes, a point also evident from the aerosol size distributions measured in the study and reported by Hand et al.⁹ Use of a $\text{PM}_{2.5}$ size cut for the URG sampling, as well as for IMPROVE samplers running at the site, leads to inclusion of a substantial portion of the lower tail of the coarse-mode size distribution in fine particle ($\text{PM}_{2.5}$) samples.

If SO_4^{2-} concentrations at Big Bend were substantially reduced, for example, because of upwind reductions in SO_2 emissions, it is likely that the resulting aerosol would be less acidic. If the SO_4^{2-} concentrations were reduced far enough, sufficient NH_3 might be present to neutralize the SO_4^{2-} in the aerosol. Further SO_4^{2-} reductions beyond this neutralization point would leave some NH_3 available to react with HNO_3 to form particulate NH_4NO_3 (assuming total N(-III) concentrations do not change in response to SO_4^{2-} decreases). Because two NH_3 molecules

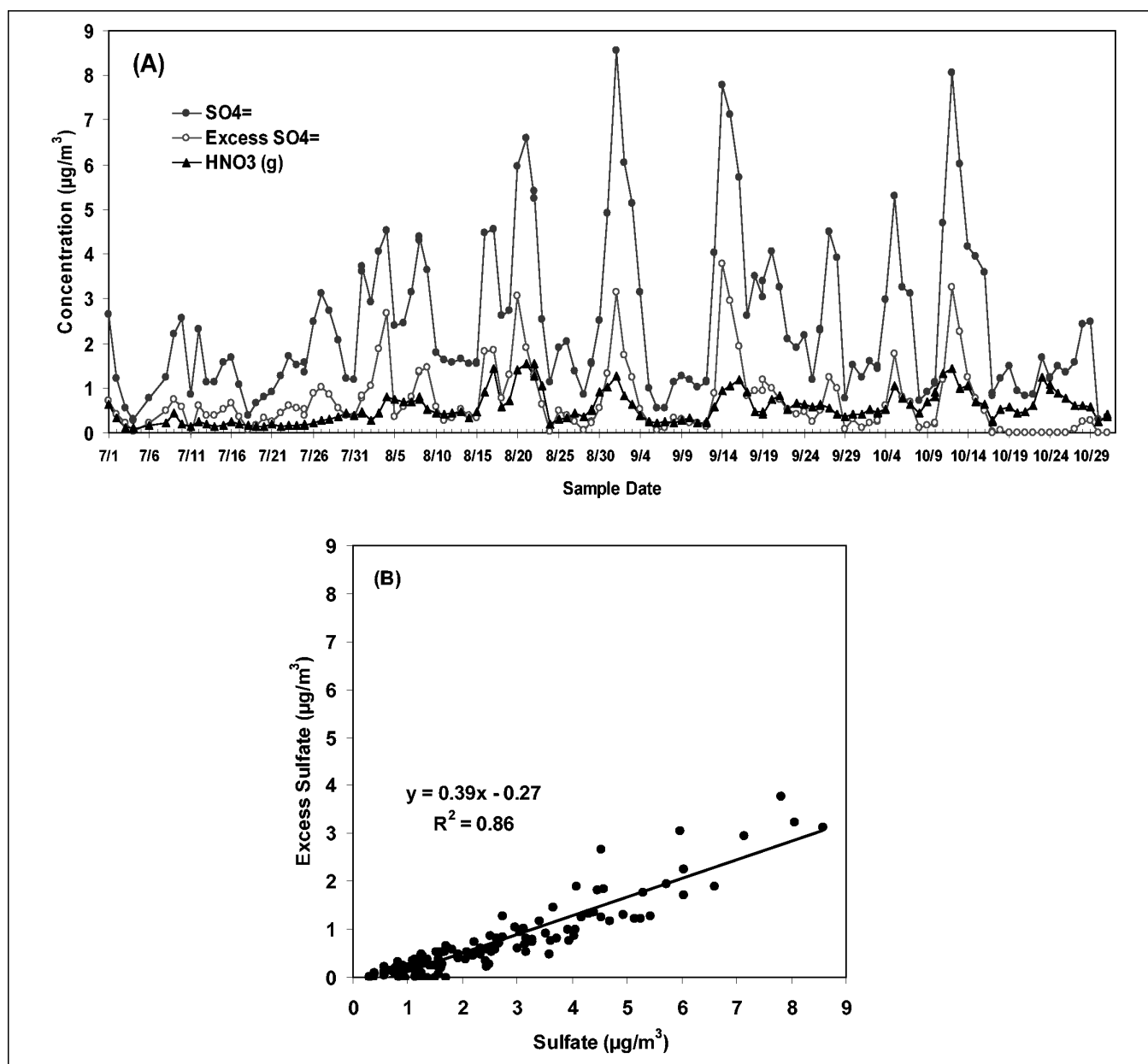


Figure 9. (a) Timelines of $\text{PM}_{2.5}$ SO_4^{2-} , excess SO_4^{2-} , and $\text{HNO}_3(\text{g})$ concentrations. (b) Relationship between excess SO_4^{2-} and SO_4^{2-} concentrations in BRAVO $\text{PM}_{2.5}$ aerosol.

are required to neutralize one SO_4^{2-} molecule, two NH_3 molecules can neutralize two HNO_3 molecules, and two NO_3^- molecules have greater mass than one SO_4^{2-} molecule, replacement of $(\text{NH}_4)_2\text{SO}_4$ by NH_4NO_3 has the potential under the right circumstances to actually produce an increase in $\text{PM}_{2.5}$ mass concentrations. West et al.²⁴ utilized model simulations of eastern U.S. aerosol composition to show that reductions in aerosol SO_4^{2-} concentrations may be up to 50% less effective in some locations at reducing annual average fine particle mass concentrations than if the role of HNO_3 is neglected. The effect was largest in winter, with up to half of the examined locations affected, but uncommon in summer because of higher temperatures that do not favor NH_4NO_3

formation. Much less is known about the potential for nonlinear responses in fine particle mass concentrations (resulting from SO_4^{2-} decreases) in western U.S. aerosol. This is in large part because of a lack of information about current western U.S. aerosol acidity and concentrations of key species including gaseous NH_3 and HNO_3 .

The BRAVO data set provides an opportunity to consider whether hypothetical reductions in regional aerosol SO_4^{2-} concentrations might be less effective at decreasing $\text{PM}_{2.5}$ mass than expected because of NH_4NO_3 formation. To consider this issue, it is useful to determine the amount of "excess" SO_4^{2-} present in BRAVO aerosol, where "excess" SO_4^{2-} is defined as the concentration of SO_4^{2-} (expressed in equivalents) minus the concentration of NH_4^+ (i.e., the

amount that SO_4^{2-} concentrations would have to be decreased for the aerosol to become neutralized, assuming particulate NH_4^+ concentrations remain unchanged). The BRAVO "excess" SO_4^{2-} timeline is shown in Figure 9A, along with timelines of $\text{PM}_{2.5}$, SO_4^{2-} and $\text{HNO}_3(\text{g})$. It is evident from the timelines that periods of high SO_4^{2-} concentration also feature high concentrations of "excess" SO_4^{2-} . This point is further made in Figure 9B where a strong correlation ($R^2 = 0.86$) is found to exist between "excess" SO_4^{2-} and SO_4^{2-} . When SO_4^{2-} concentrations are high, "excess" SO_4^{2-} concentrations are also high, indicating that considerable reductions in aerosol SO_4^{2-} concentrations could be made on these days before the aerosol became neutralized. Second, the high temperatures present during the summer and fall at Big Bend do not favor formation of NH_4NO_3 , even if additional gaseous NH_3 is made available by SO_4^{2-} reductions. Last, even if all the available gaseous nitric were shifted to the particulate phase, the additional mass (see Figure 9A) would still be smaller during most periods than the SO_4^{2-} concentration decreases required to neutralize the aerosol. Accordingly, it appears that during summer and fall at Big Bend, SO_4^{2-} concentrations could be significantly decreased without much concern about nonlinear responses in fine particle mass concentrations.

ACKNOWLEDGMENTS

The authors thank D.E. Sherman, M.P. Hannigan, J.L. Hand, and J.E. Reilly for their contributions to the success of the field campaign. They are grateful to Air Resource Specialists for excellent field support before and during the campaign and to W. Malm for numerous helpful discussions. This study was funded by the National Park Service, grants CA238099001 TO 01-52 and CA238099001 TO 01-54. However, the results, findings, and conclusions expressed in this paper are solely those of the authors and are not necessarily endorsed by the management, sponsors, or collaborators of the BRAVO study. A comprehensive final report for the BRAVO study is anticipated in 2004.

REFERENCES

- Gebhart, K.A.; Malm, W.C.; Flores, M. A Preliminary Look at Source-Receptor Relationships in the Texas-Mexico Border Area; *J. Air & Waste Manage. Assoc.* **2000**, *50*, 858-868.
- Spatial and Seasonal Patterns and Temporal Variability of Haze and its Constituents in the United States: Report III*; IMPROVE report; Cooperative Institute for Research in the Atmosphere: Fort Collins, CO, May 2000.
- Spatial and Seasonal Patterns and Long Term Variability of the Composition of the Haze in the United States: An Analysis of Data from the IMPROVE Network*; IMPROVE report; Cooperative Institute for Research in the Atmosphere: Fort Collins, CO, July 1996.
- Gebhart, K.A.; Kreidenweis, S.M.; Malm, W.C. Back-Trajectory Analyses of Fine Particulate Matter Measured at Big Bend National Park in the Historical Database and the 1996 Scoping Study; *Sci. Total Environ.* **2001**, *276* (1-3), 185-204.
- Day, D.E.; Malm, W.C.; Kreidenweis, S.M. Aerosol Light Scattering Measurements as a Function of Relative Humidity; *J. Air & Waste Manage. Assoc.* **2000**, *50*, 710-716.

- Malm, W.C.; Day, D.E.; Kreidenweis, S.M. Light Scattering Characteristics of Aerosols as a Functions of Relative Humidity, Part I, A Comparison of Measured Scattering and Aerosol Concentrations Using the Theoretical Models; *J. Air & Waste Manage. Assoc.* **2000**, *50*, 686-700.
- Malm, W.C.; Day, D.E. Estimates of Aerosol Species Scattering Characteristics as a Function of Relative Humidity; *Atmos. Environ.* **2001**, *35*, 2845-2860.
- Kreidenweis, S.M.; Remer, L.A.; Bruintjes, R.; Dubovik, O. Smoke Aerosol from Biomass Burning in Mexico: Hygroscopic Smoke Optical Model; *J. Geophys. Res.* **2001**, *106* (D5), 4831-4844.
- Hand, J.L.; Kreidenweis, S.M.; Sherman, D.E.; Collett, J.L.; Hering, S.V.; Day, D.E.; Malm, W.C. Aerosol Size Distributions and Visibility Estimates during the Big Bend Regional Aerosol and Visibility Observational (BRAVO) Study; *Atmos. Environ.* **2002**, *36*, 5043-5055.
- Brown, S.G.; Herckes, P.; Hannigan, M.P.; Kreidenweis, S.M.; Collett, J.L. Characterization of Organic Aerosol in Big Bend National Park, Texas; *Atmos. Environ.* **2002**, *36*, 5807-5818.
- Perrino, C.; Santis, F.D.; Febo, A. Criteria for the Choice of a Denuder Sampling Technique Devoted to the Measurement of Atmospheric Nitrous and Nitric Acids; *Atmos. Environ.* **1990**, *24A*, 617-626.
- Marple, V.A.; Rubow, K.L.; Behm, S.M.A. Microorifice Visibility Deposit Impactor (MOUDI): Description, Calibration, and Use; *Aerosol Sci. Technol.* **1991**, *14*, 434-446.
- Lee, T.; Collett, J.L. *The Ionic Composition of Aerosol in Big Bend National Park*; Cooperative Institute for Research in the Atmosphere: Fort Collins, CO, 2002.
- Koutrakis, P.; Wolfson, J.M.; Slater, J.L.; Brauer, M.; Spengler, J.D.; Stevens, R. K.; Stone, C. L. Evaluation of an Annular Denuder/Filter Pack System to Collect Acidic Aerosols and Gases; *Environ. Sci. Technol.* **1988**, *22* (12), 1463-1467.
- Koutrakis, P.; Wolfson, J.M.; Spengler, J.D. An Improved Method of Measuring Aerosol Strong Acidity: Results from a Nine-Month Study in St. Louis, Missouri, and Kingston, Tennessee; *Atmos. Environ.* **1988**, *22*, 157-162.
- Spengler, J.D.; Keeler, G.J.; Koutrakis, P.; Ryan, P.B.; Raizenne, M.; Franklin, C.A. Exposures to Acidic Aerosols; *Environ. Health Perspect.* **1989**, *79*, 43-51.
- Lee, H.S.; Wadden, R.A.; Scheff, P.A. Measurement and Evaluation of Acid Air Pollutants in Chicago Using an Annular Denuder System; *Atmos. Environ.* **1993**, *27A*, 543-553.
- Spengler, J.D.; Brauer, M.; Koutrakis, P. Acid Air and Health; *Environ. Sci. Technol.* **1990**, *24* (7), 946-956.
- Brauer, M.; Koutrakis, P.; Keeler, G.J.; Spengler, J.D. Indoor and Outdoor Concentration of Inorganic Acidic Aerosols and Gases; *J. Air & Waste Manage. Assoc.* **1991**, *41* (2), 171-181.
- Cheng, Z.L.; Lam, K.S.; Chan, L.Y.; Wang, T.; Cheng, K.K. Chemical Characteristics of Aerosols at Coastal Station in Hong Kong. I. Seasonal Variation of Major Ions, Halogens and Mineral Dusts between 1995 and 1996; *Atmos. Environ.* **2000**, *34*, 2771-2783.
- Seinfeld, J.H.; Pandis, S.N. *Atmospheric Chemistry and Physics*; Wiley & Sons: New York, 1998.
- Krueger, B.J.; Grassian, V.H.; Laskin, A.; Cowin, J.P. The Transformation of Solid Atmospheric Particles into Liquid Droplets through Heterogeneous Chemistry: Laboratory Insights into the Processing of Calcium Containing Mineral Dust Aerosol in the Troposphere; *Geophys. Res. Lett.* **2003**, *30*, 1148.
- Malm, W.C.; Day, D.E.; Kreidenweis, S.M.; Collett, J.L.; Lee, T. Humidity-Dependent Optical Properties of Fine Particles during the Big Bend Regional Aerosol and Visibility Observational Study; *J. Geophys. Res.* **2003**, *108* (D9), 4279.
- West, J.J.; Ansari, A.S.; Pandis, S.N. Marginal $\text{PM}_{2.5}$: Nonlinear Aerosol Mass Response to Sulfate Reductions in the Eastern United States; *J. Air & Waste Manage. Assoc.* **1999**, *49*, 1415-1424.

About the Authors

Taehyoung Lee is a Ph.D. student in the Department of Atmospheric Science at Colorado State University in Fort Collins, CO, where he received an M.S. in 2002. Dr. Sonia M. Kreidenweis and Dr. Jeffrey L. Collett, Jr., are professors in the Department of Atmospheric Science at Colorado State University. Address correspondence to: Jeffrey L. Collett, Jr., Department of Atmospheric Science, Colorado State University, Fort Collins, CO 80523; fax: (970) 491-8449; e-mail: collett@lamar.colostate.edu.